Coastal Ocean Mixing and Advection During Hurricane Sandy and Arthur

Travis Miles, Greg Seroka, and Scott Glenn
Rutgers, The State University of New Jersey
Department of Marine and Coastal Sciences
Center for Ocean Observing Leadership
New Brunswick, New Jersey
tnmiles@marine.rutgers.edu

***Abstract*— The Mid Atlantic Bight continental shelf has one of the largest summer temperature gradients in the world, with near bottom temperatures below 8C and peak surface temperatures over 28C. This is largely due to the summer Cold Pool, remnant winter water that is generated on the northern MAB and transported southward along the continental shelf in spring and early summer. During tropical cyclones that impact the MAB continental shelf, such as Hurricane Irene in 2011, shear driven mixing of Cold Pool water across the thermocline has the potential to cool the oceans surface and reduce storm intensity. In this study we compare coastal ocean advection and mixing processes during Hurricane Sandy and Hurricane Arthur, an offshore tracking tropical cyclone in the summer of 2014, to demonstrate the range of potential storm impacts on the coastal ocean of the MAB. To perform this analysis we use data from advanced Slocum autonomous underwater glider deployments in each storm as well as the Regional Ocean Modeling System (ROMS).**

Keywords*— *Coastal storms, ocean observing systems, autonomous underwater vehicles, coastal ocean modeling.

I. INTRODUCTION

The Mid Atlantic Bight continental shelf has one of the largest summer temperature gradients in the world, with near bottom temperatures below 8C and peak surface temperatures over 28C. This is largely due to the summer Cold Pool [1], remnant winter water that is generated on the northern MAB and transported southward along the continental shelf in spring and early summer. During tropical cyclones that impact the MAB continental shelf, such as Hurricane Irene in 2011, shear driven mixing of Cold Pool water across the thermocline has the potential to cool the oceans surface and reduce storm intensity [2]. While this process was observed in detail from a networked coastal ocean observatory in Hurricane Irene, a coupled ocean-atmosphere model study has shown the ocean to have a limited impact on Hurricane Sandy in 2012 [3].

In this study we compare coastal ocean advection and mixing processes during Hurricane Sandy and Hurricane Arthur, an offshore tracking tropical cyclone in the summer of 2014. Hurricane sandy was a late-season tropical cyclone that crossed the New Jersey shelf in late October, when stratification had already partially broken down for the season. Hurricane Arthur was one of the earliest tropical cyclones to make landfall in North Carolina in early July prior to crossing the southern portion of the Mid-Atlantic Bight, when stratification was at its highest. With vastly different trajectories and shelf stratification conditions they demonstrate the range of potential storm impacts on the coastal ocean of the MAB. To perform this analysis we use data from advanced Slocum autonomous underwater gliders deployed ahead ofeach storm as well as the Regional Ocean Modeling System (ROMS).

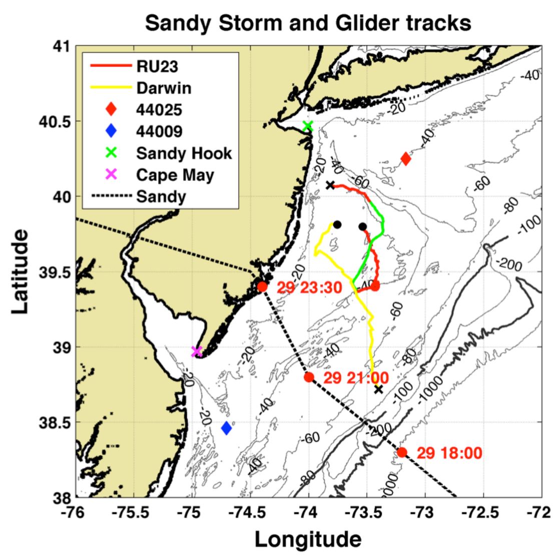

Figure 1 Map of the NJ Shelf with the dashed line representing Hurricane Sandy's onshore track (times in GMT). Glider RU23 (red) and it's storm sampling period represented in Figure 2 (green). A second glider, Darwin (yellow), is also plotted.

II. METHODS

Teledyne-Webb Research Slocum gliders are buoyancy driven autonomous underwater vehicles that are mobile profiling sensor platforms, with interchangeable science bays [Schofield et al., 2007; Schofield et al., 2010]. Gliders have a proven history of sampling in extreme weather conditions, [4]–[7]. A Slocum G1 glider, RU23 was deployed

978-0-933957-43-5 ©2015 MTS

ahead of Hurricane Sandy in October 2012, while a specially designed G2 Storm glider RU30 was deployed ahead of Hurricane Arthur in July of 2014. RU23 and RU30 were equipped with Seabird Electronics (SBE) un-pumped and pumped conductivity temperature and depth (CTD) sensors, respectively. Both gliders were equipped with two Wetlabs Eco-triplets that measured chlorophyll fluorescence, colored dissolved organic matter (CDOM), and four channels of optical backscatter.

To measure water-column currents Nortek Aquadopp current profilers with custom glider heads were externally mounted in an upward looking position and logged data internally. The Aquadopps were configured to collect data in beam coordinates in one meter bins with a beam length of ten meters every two seconds. On downcasts with a glider pitch angle of 26.5 degrees the Aquadopps had a pitch angle of 0 degrees. We emply a shear-least squares method originally detailed for lowered current profilers [8] and adapted for use on autonomous platforms [9]. We calculate water column shear at one meter intervals on downcasts only and use a combination of pitch angle, heading and depth, known as dead-reckoning [10] to calculate the mean water-column velocity.

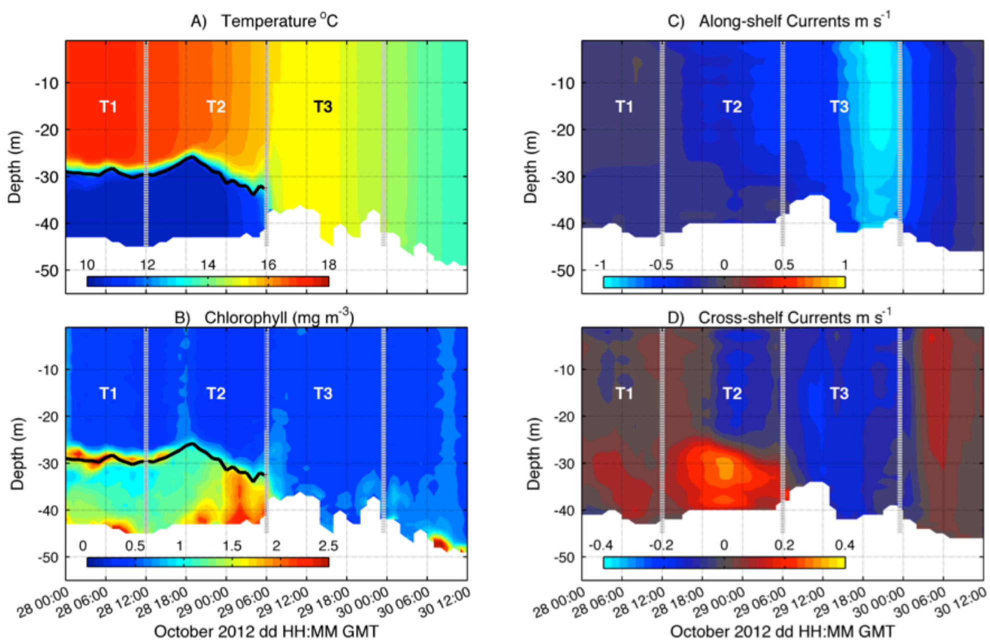

Figure 2 RU23 glider data during the storm forcing period on October 28th at 00:00 GMT to the 30th at 12:00 GMT (represented by the black line in Figure 1). A) Temperature and B) Chlorophyl (mg/m3) with a black contour representing the thermocline. C) Along-shelf and D) cross-shelf de-tided currents calculated from the Nortek Aquadopp current profiler. Positive is toward the southwest and offshore in the along- and cross- shelf directions respectively. Note the different colorbar between the along and cross- shelf currents.

ROMS is a three-dimensional sigma coordinate numerical ocean model [11]–[13] that is commonly used for coastal and regional model applications. The Experimental System for Predicting Shelf and Slope Optics (ESPreSSO) setup [14]–[18] used here covers from Cape Hatteras to Cape Cod, and near shore to beyond the shelf-break. The system has an approximately 5 km horizontal resolution, 36 vertical levels and a 6-minute time step with model data output hourly. Boundary conditions are derived from the HYCOM-NCODA (http://hycom.org/) and tides derived from the ADCIRC tidal model (http://adcirc.org/). For the Sandy case the model is initialized from the original assimilative ESPreSSO 4-dimensional variational data assimilations (IS4DVAR) output on October 25th and run forward. Atmospheric forcing is from the Rutgers University Weather Research and Forecast model setup described in detail in [7]. The ESPreSSO model has been used extensively on the MAB for a range of applications including for sediment transport studies during Hurricane Sandy on the MAB[7].

III. Results

A. Hurricane Sandy

Hurricane Sandy developed as a late-season tropical wave off the coast of Africa on October 11th 2012. On October 24th the cyclone made landfall as a category 1 hurricane in Jamaica and continued to make landfall in Cuba as a category 3 on October 25th. The cyclone left the Caribbean the storm turned toward the northeast again as a category one hurricane. During this period, as the storm passed to the east of North Carolina, the radius of maximum winds covered approximately 180 kilometers. Early on October 29th Sandy took a sharp left turn toward the NY/NJ coastline. After a brief re-intensification period as the storm crossed the continental shelf it interacted with cooler waters and a cold air mass over the eastern United States, ultimately transitioning to extra-tropical at 2100 GMT on October 29th just prior to landfall at 2330 GMT near Brigantine, New Jersey. This storm drove extensive storm surge along the NY/NJ coastlines and resulted in over $68 Billion in damages[19].

Glider RU23 was deployed 15 km southeast of Sandy Hook, NJ on October 25th, (Figure 1) as forecasts indicated Sandy would approach the MAB. The glider was piloted due east to the 40 meter isobath in order to sample the coastal ocean at a safe distance from the coastline. Cross-sections of RU23 temperature and currents (Figure 2) show three distinct time periods based on the evolution of the thermocline, which we refer to as T1, T2 and T3.The initial stratified period T1 was between 00:00 and 12:00 GMT on October 28th and showed warm surface temperatures of over 17°C consistent with pre-storm conditions sampled by Darwin and a sharp thermocline at 25 meters depth. Below the thermocline temperatures were 10°C and uniform to the bottom. During T1 de-tided along-shelf surface currents were weak and southwestward with flow below 0.1 m s^{-1}, while the lower layer showed bottom intensified flow over 0.2 m s^{-1}. There was slight onshore flow near the surface and offshore flow near the bottom of ~ 0.1 m s^{-1}. During T2 between 12:00 GMT on the 28th and 06:00 GMT on the 29th (Figure 2) the thermocline initially rose and then deepened dramatically, reaching the bottom in twelve hours. Along-shore currents increased to over 0.6 m s^{-1} in the surface layer and remained near 0.2 m s^{-1} in the bottom similar to the initial stratified phase. In the cross-shelf direction currents were onshore in the surface as along-shore surface winds, which had now persisted for over an inertial period (~18 hours), spun up the surface

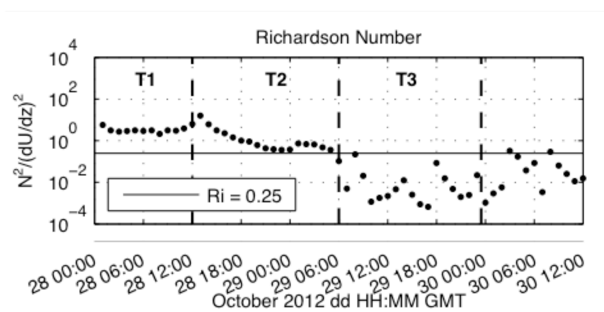

Figure 4 Bulk Richardson number calculated from equation 1 along the glider track. The horizontal black line represents Ri of 0.25.

Ekman layer. Cross-shelf flow in the lower layer was offshore and over 0.5 m s^{-1} at 20:00 GMT on the 28th. Surface temperatures dropped gradually, despite a sharp increase in bottom temperatures of 4°C in two hours as the thermocline deepened. In T3, between the 29th at 06:00 GMT and landfall on the 29th 23:30 GMT the watercolumn transitioned from a two- to one- layer system (Figure 2). Cross-shelf circulation shut down and currents rotated to be along-shelf and uniform throughout the watercolumn, with peak values over 1 m s^{-1} as the eye of Sandy crossed the shelf. Full watercolumn temperatures continued to gradually decrease until they dropped below 13C after eye passage

Two-layer cross-shelf flow during the deepening phase between 12:00 GMT on the 28th and 06:00 GMT on the 29th was consistent with the seaward side of a downwelling front, while single-layer flow was consistent with the shoreward side of a downwelling front similar to results discussed in [Lentz, 2001] and [Austin and Lentz, 2002]. Along-shelf displacement of the glider was over 50 km, but piloting to maintain cross-shelf position and two-layer flow limited cross-shelf displacement during T2 and T3, thus the glider likely sampled the shoreward and seaward sides of the downwelling front, in T2 and T3 respectively, as it was advected past the glider in the offshore direction. Bulk Richardson numbers from:

$$Ri = N2/(\partial u \; \partial z) \qquad (1)$$

where N^2 is the hourly averaged water-column buoyancy frequency across the thermocline, and $(\partial u \; \partial z)^2$ is the hourly averaged maximum shear across the thermocline calculated from the Aquadopp. Studies have shown [20], [21] that the water column is stable (unstable) when Richardson number is above (below) a critical number (Rc) of 0.25. Richardson numbers (Figure 3) were greater than 0.25 until the 29th at 06:00 after the thermocline had already deepened

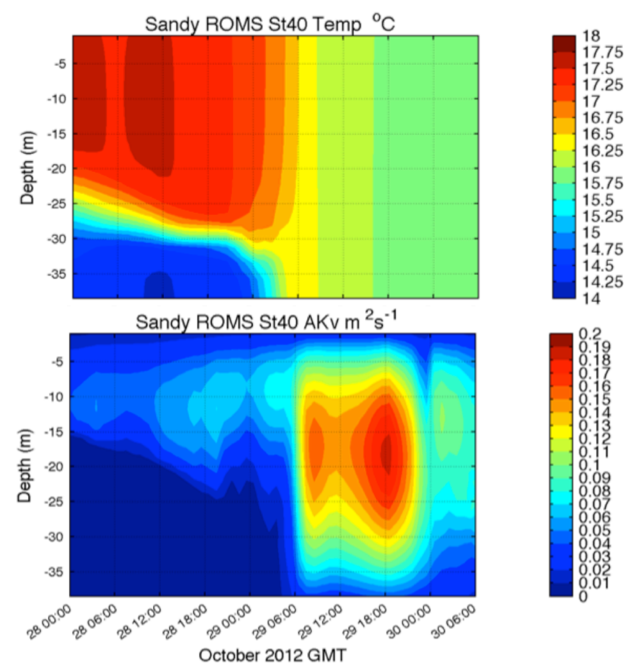

Figure 3 Cross sections of temperature (upper) and eddy diffusivity at the 40 meter isobaths in the ROMS model near the glider position.

approximately 5 meters.

A cross section of the storm time period from ROMS near the glider location on the 40 meter isobaths (Figure 4) shows similar stratification with a few differences. Bottom waters were approximately ~3°C warmer prior to the storm and the thermocline was deeper and slightly more diffuse. Similar deepening of the thermocline occurred ahead between

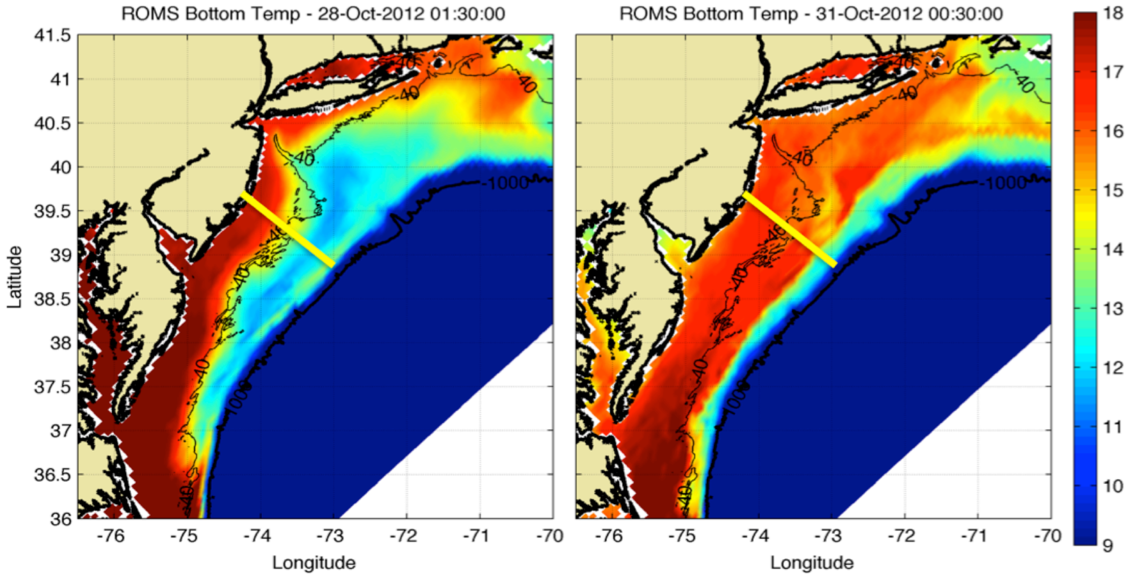

Figure 5 Bottom temperatures from the ESPreSSO ROMS model before (left panel) and after (right panel) eye passage.

the 28th at 00:00 GMT and the 29th at 06:00 GMT, followed by a transition from two-layers to one-layer (Figure 4). Eddy diffusivities were relatively low in prior to the 29th at 06:00 GMT with limited increases in the surface layer indicating limited mixing across the thermocline. Eddy diffusivities increase dramatically after the transition from a one- to two-layer system supporting the argument that advection was responsible for the transition rather than mixing (Figure 4). From a shelf-wide perspective bottom temperatures inshore of the 40 meter isobaths were near 18^{o}C indicating a well-mixed nearshore region. Bottom temperatures offshore of the 40 meter isobaths pre-storm are near ~13^{o}C across (Figure 5) the majority of the shelf. After the storm the warm bottom temperatures found inshore extend nearly to the shelf-break, with a total offshore advection of ~30 km.

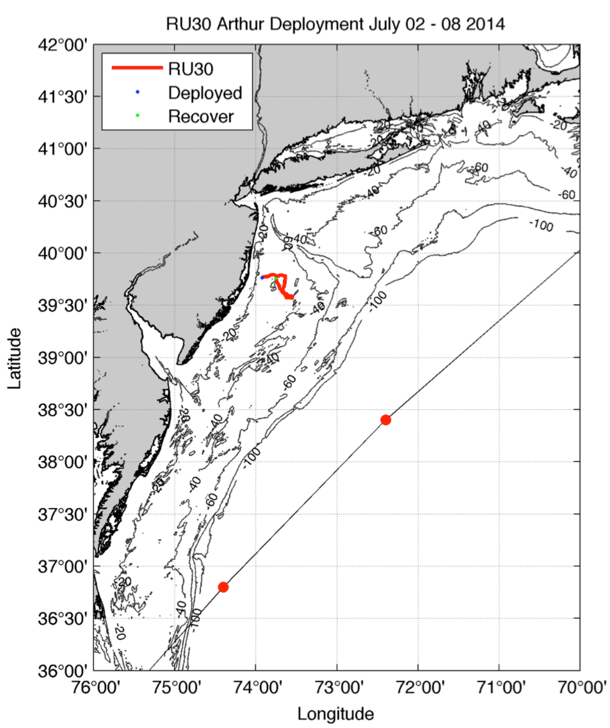

Figure 6 Map of the MAB with Hurricane Arthurs track (black with red dots), the glider track (red line).

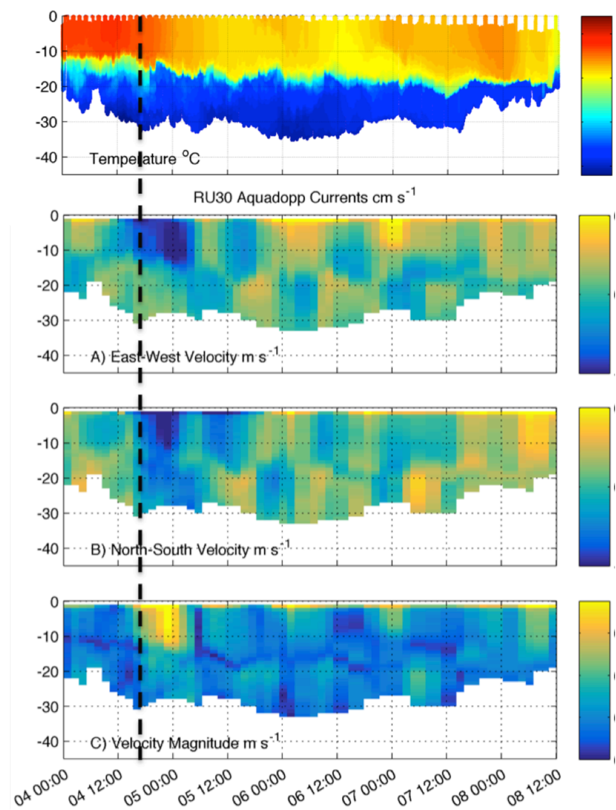

Figure 7 Cross-sections of glider RU30 temperature and velocity components and magnitude. Vertical black line denotes time of storm passage.

B. Hurricane Arthur

Hurricane Arthur developed east of Florida on July 1st when a depression that had crossed from the Gulf of

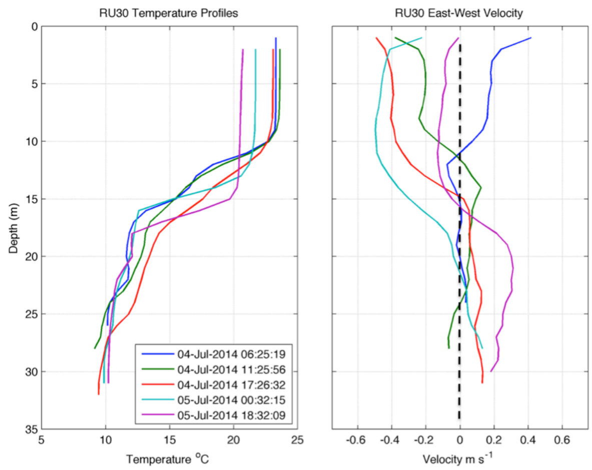

Figure 8 RU30 segment averaged profiles of temperature (left panel) and east-west velocity (right panel).

Mexico into the South Atlantic bight interacted with a region of mid-level anticyclone over the Western Atlantic. This interaction caused Arthur to accelerate northward rapidly throughout July 2nd and 3rd. The hurricane strengthened as it passed east of Savannah Georgia and eventually reached peak intensity off the coast of Cape Fear, North Carolina. After crossing the Outer Banks, Arthur accelerated northeastward over the western Atlantic east of the Mid-Atlantic until it weakened into a tropical storm on July 5th east of Provincetown, Massachusetts.

RU30 was deployed as part of a NOAA Cooperative Institute for the North Atlantic region (CINAR) Tempests project on July 3rd 2014 out of Tuckerton, NJ (Figure 6). The glider was piloted due east toward the 40 meter isobath similar to RU23 in Sandy. As Arthur was a fast moving storm the glider was only in the field for approximately 18 to 24 hours before experiencing outer edge winds from the storm. Initially on July 4th at 00:00 GMT the watercolumn (Figure 7) was highly stratified typical of summer conditions on the MAB. Surface temperatures were near 23 to 24^{o}C, bottom temperatures were near 10^{o}C and there was a shallow thermocline at 10 meters depth. Segment averaged profiles (mean profiles between each glider surfacing) between July 4th at 06:25 GMT and July 5th at 18:32 show limited cooling of only about 0.5^{o}C over the first 12 hours in the surface layer. Despite the limited surface cooling the thermocline deepened and grew less sharp by the end of July 4th at 17:26 GMT. After this first 12-hour period surface temperatures dropped over 3^{o}C and the thermocline lowered to 15 meters depth (Figure 8). Profiles of the east and west current velocities during this same period show maximum vertical shear starting on July 4th at 17:26 GMT with westward surface velocities and low near-bottom velocities.

After the eye passed the surface currents continue to rotate for a number of days after. Wavelet spectral analysis of the surface currents (Figure 9) shows the surface currents oscillating with a period of near 18 hours, near the local inertial period, that slowly lengthens with time. This suggests that any additional cooling is likely due to inertial surface currents driving intermittent shear driven mixing across the thermocline. Further analysis of glider data and ROMS modeling are underway in order to confirm this result.

IV. Discussion & Conclusion

RU23 and RU30 were deployed off the MAB continental shelves in response to Hurricanes Sandy and Arthur respectively. The storms had vastly different tracks, speeds, and struck at the far extremes of the Atlantic Hurricane season with different stratification regimes. Thus they represent two very different coastal ocean responses to summer storms on the MAB. Sandy struck during the late season fall transition period between summer and winter, thus temperatures were lower and the thermocline deeper than typically occurs on the shelf. The onshore track and large size of the storm drove large volumes of water above the thermocline onshore leading to a downwelling circulation that ultimately advected the bottom Cold Pool offshore nearly 30 kilometers. The limited mixing observed by the glider and model output support this finding. Previous studies have identified this type of circulation for persistent downwelling

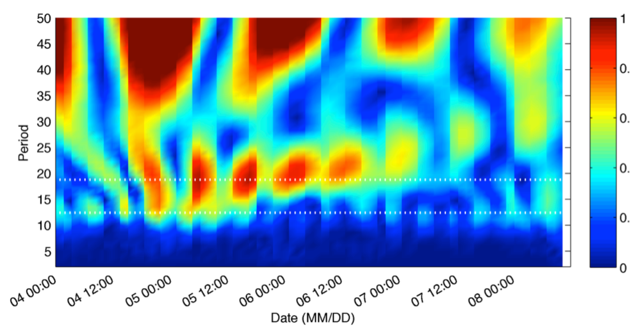

Figure 9 Wavelet spectrum of glider RU30 surface currents.

favorable winds, with deeper thermoclines resulting in more advection than shallower thermoclines [22], [23].

Hurricane Arthur, with its fast moving offshore track, and enhanced stratification did not setup advective downelling circulation on the MAB shelf. Rather the storm had limited direct mixing prior to eye-passage and enhanced mixing behind the eye during the post-storm inertial response. The shallower thermocline was more conducive to direct wind-forced mixing. Further analysis of these two storms, as well as Hurricane Irene are ongoing and provide a broad view of the three-dimensional processes that occur on the stratified MAB continental shelf during summer tropical cyclones.

The dynamic ocean response to these two storms indicates that fully coupled three-dimensional ocean and atmosphere models may be necessary to resolve changes to the surface ocean and further investigate the impact of the coastal ocean on atmospheric forecasts of hurricane intensity in the MAB. Further observational assets such as gliders and moorings should be included in data assimilation for these models to improve the accuracy the modeled ocean ahead of and during storm events. Future observational work will include downward looking current profilers to more accurately measure bottom stress, and accelerometers to resolve wave motions at glider locations.

V. Acknowledgements

Glider data used in this study is available through the MARACOOS assets page http://maracoos.org/data and http://marine.rutgers.edu/cool/auvs/index.php?did=369 with more detailed datasets available upon request to tnmiles@marine.rutgers.edu. Regional Ocean Modeling System and WRF model results are also available upon request to tnmiles@marine.rutgers.edu. Buoy data and WaveWatch III datasets are publicly available through http://www.ndbc.noaa.gov/ and http://polar.ncep.noaa.gov, respectively. We are grateful for the funding support provided by NOAA Grant NA11NOS0120038 as part of MARACOOS, the regional partner of U.S. IOOS and NOAA Grant NA13OAR4830233 as part of CINAR, the regional partner of the CIPO. We would also like to thank Teledyne-Webb Research for providing graduate student funding, NortekUSA for providing equipment through a student equipment grant.

VI. References

[1] R. W. Houghton, R. Schlitz, R. C. Beardsley, B. Butman, and J. L. Chamberlin, "The Middle Atlantic Bight Cold Pool: Evolution of the Temperature Structure During Summer 1979," *J. Phys. Oceanogr.*, vol. 12, no. 10, pp. 1019–1029, Oct. 1982.

[2] S. Glenn, D. Aragon, L. Bowers, M. Crowley, R. Dunk, C. Evans, C. Haldeman, E. Handel, T. Haskins, J. Kerfoot, J. Kohut, J. Levin, T. Miles, L. Palamara, H. Roarty, O. Schofield, G. Seroka, M. Smith, N. Strandskov, J. Wilkin, Y. Xu, J. Zavala-Garay, C. Thoroughgood, G. Kuska, B. Lipphardt, M. Oliver, M. Shatley, W. Brown, A. Gongopadhyay, C. Jakubiak, A. Schmidt, E. Howlett, D. Ullman, J. O'Donnell, T. Fake, N. Georgas, A. Blumberg, M. Bruno, T. Herrington, W. Boicourt, T. Wazniak, J. Titlow, R. Toll, L. Atkinson, T. Updyke, N. Verona, H. Seim, and M. Muglia, "Process-driven improvements to hurricane intensity and storm surge forecasts in the mid-atlantic bight: Lessons learned from hurricanes irene and sandy," in *OCEANS 2013 MTS/IEEE Bergen: The Challenges of the Northern Dimension*, 2013.

[3] J. B. Zambon, R. He, and J. C. Warner, "Tropical to extratropical: Marine environmental changes associated with SuperstormSandy prior to its landfall," *Geophys. Res. Lett.*, vol. 41, pp. 8935–8943, 2014.

[4] S. Glenn, C. Jones, M. Twardowski, L. Bowers, J. Kerfoot, J. Kohut, D. Webb, and O. Schofield, "Glider observations of sediment resuspension in a Middle Atlantic Bight fall transition storm," *Limnol. Oceanogr.*, vol. 53, no. 5 part 2, pp. 2180–2196, 2008.

[5] T. Miles, S. Glenn, and O. Schofield, "Temporal and spatial variability in fall storm induced sediment resuspension on the Mid-Atlantic Bight," *Cont. Shelf Res.*, vol. 63, 2013.

[6] S. Ruiz, L. Renault, B. Garau, and J. Tintoré, "Underwater glider observations and modeling of an abrupt mixing event in the upper ocean," *Geophys. Res. Lett.*, vol. 39, no. 1, p. n/a–n/a, Jan. 2012.

[7] T. Miles, G. Seroka, J. Kohut, O. Schofield, and S. Glenn, "Glider observations and modeling of sediment transport in Hurricane Sandy," *J. Geophys. Res. Ocean.*, p. n/a–n/a, Feb. 2015.

[8] M. Visbeck, "Deep Velocity Profiling Useding Lowered Acoustic Doppler Current Profilers: Bottom Track and Inverse Solutions," *J. Atmos. Ocean. Technol.*, 2002.

[9] R. E. Todd, D. L. Rudnick, M. R. Mazloff, R. E. Davis, and B. D. Cornuelle, "Poleward flows in the southern California Current System: Glider observations and numerical simulation," *J. Geophys. Res.*, vol. 116, no. C2, p. C02026, Feb. 2011.

[10] R. Davis, C. Eriksen, and C. Jones, "Autonomous Buoyancy-driven Underwater Gliders," in *Technology and Applications of Autonomous Underwater Vehicles*, G. Griffiths, Ed. Taylor & Francis, 2003, p. 37.

[11] A. F. Shchepetkin and J. C. McWilliams, "The regional oceanic modeling system (ROMS): a split-explicit, free-surface, topography-following-coordinate oceanic model," *Ocean Model.*, vol. 9, no. 4, pp. 347–404, Jan. 2005.

[12] A. F. Shchepetkin and J. C. McWilliams, "Correction and commentary for 'Ocean forecasting in terrain-following coordinates: Formulation and skill assessment of the regional ocean modeling system' by Haidvogel et al., J. Comp. Phys. 227, pp. 3595–3624," *J. Comput. Phys.*, vol. 228, no. 24, pp. 8985–9000, Dec. 2009.

[13] D. B. Haidvogel, H. Arango, W. P. Budgell, B. D. Cornuelle, E. Curchitser, E. Di Lorenzo, K. Fennel, W. R. Geyer, A. J. Hermann, L. Lanerolle, J. Levin, J.

C. McWilliams, A. J. Miller, A. M. Moore, T. M. Powell, A. F. Shchepetkin, C. R. Sherwood, R. P. Signell, J. C. Warner, and J. Wilkin, “Ocean forecasting in terrain-following coordinates: Formulation and skill assessment of the Regional Ocean Modeling System,” *J. Comput. Phys.*, vol. 227, no. 7, pp. 3595–3624, Mar. 2008.

[14] K. Fennel, J. Wilkin, J. Levin, J. Moisan, J. O’Reilly, and D. Haidvogel, “Nitrogen cycling in the Middle Atlantic Bight: Results from a three-dimensional model and implications for the North Atlantic nitrogen budget,” *Global Biogeochem. Cycles*, vol. 20, no. 3, p. n/a–n/a, Sep. 2006.

[15] B. Cahill, O. Schofield, R. Chant, J. Wilkin, E. Hunter, S. Glenn, and P. Bissett, “Dynamics of turbid buoyant plumes and the feedbacks on near-shore biogeochemistry and physics,” *Geophys. Res. Lett.*, vol. 35, no. 10, p. L10605, May 2008.

[16] W. G. Zhang, J. L. Wilkin, J. C. Levin, and H. G. Arango, “An Adjoint Sensitivity Study of Buoyancy- and Wind-Driven Circulation on the New Jersey Inner Shelf,” *J. Phys. Oceanogr.*, vol. 39, no. 7, pp. 1652–1668, Jul. 2009.

[17] W. G. Zhang, J. L. Wilkin, and R. J. Chant, “Modeling the Pathways and Mean Dynamics of River Plume Dispersal in the New York Bight,” *J. Phys. Oceanogr.*, vol. 39, no. 5, pp. 1167–1183, May 2009.

[18] J. L. Wilkin and E. J. Hunter, “An assessment of the skill of real-time models of Mid-Atlantic Bight continental shelf circulation,” *J. Geophys. Res. Ocean.*, vol. 118, no. 6, pp. 2919–2933, Jun. 2013.

[19] E. S. Blake, T. B. Kimberlain, R. J. Berg, P. C. John, and J. L. Beven II, “Tropical Cyclone Report: Hurricane Sandy,” *Natl. Hurric. Cent.*, vol. 12, 2013.

[20] R. J. Chant, W. R. Geyer, R. Houghton, E. Hunter, and J. Lerczak, “Estuarine Boundary Layer Mixing Processes: Insights from Dye Experiments*,” *J. Phys. Oceanogr.*, vol. 37, no. 7, pp. 1859–1877, Jul. 2007.

[21] J. H. Trowbridge, “A simple description of the deepening and structure of a stably stratified flow driven by a surface stress,” *J. Geophys. Res. Ocean.*, vol. 97, no. C10, pp. 15529–15543, Oct. 1992.

[22] J. Austin and S. Lentz, “The inner shelf response to wind-driven upwelling and downwelling.,” *J. Phys. Oceanogr.*, no. 1905, pp. 2171–2193, 2002.

[23] S. Lentz, “The Influence of Stratification on the Wind-Driven Cross-Shelf Circulation over the North Carolina Shelf*,” *J. Phys. Oceanogr.*, no. Lentz 1995, pp. 2749–2760, 2001.